ACS APPLIED MATERIALS & INTERFACES

www.acsami.org

Research Article

Triglyceride-Tethered Membrane Lipase Sensor

Upeksha Mirissa Lankage, Stephen A. Holt, Samara Bridge, Bruce Cornell, and Charles G. Cranfield*

Cite This: *ACS Appl. Mater. Interfaces* 2023, 15, 52237−52243

Read Online

ACCESS | Metrics & More | Article Recommendations | Supporting Information

ABSTRACT: Sensors that can quickly measure the lipase activity from biological samples are useful in enzyme production and medical diagnostics. However, current lipase sensors have limitations such as requiring fluorescent labels, pH control of buffer vehicles, or lengthy assay preparation. We introduce a sparsely tethered triglyceride substrate anchored off of a gold electrode for the impedance sensing of real-time lipase activity. The tethered substrate is self-assembled using a rapid solvent exchange technique and can form an anchored bilayer 1 nm off the gold electrode. This allows for an aqueous reservoir region, providing access to ions transported through membrane defects caused by triglyceride enzymatic hydrolysis. Electrical impedance spectroscopy techniques can readily detect the decrease in resistance caused by enzymatically induced defects. This rapid and reliable lipase detection method can have potential applications in disease studies, monitoring of lipase production, and as point-of-care diagnostic devices.

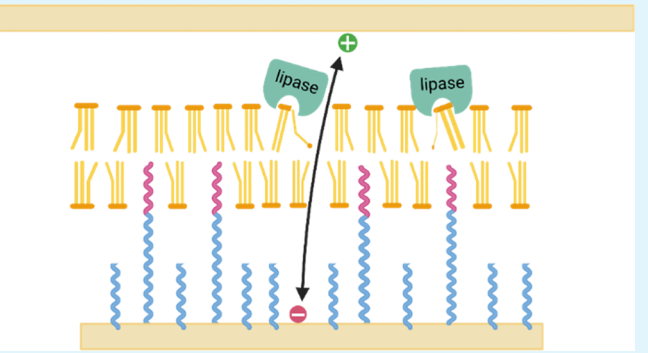

KEYWORDS: *tethered lipid membranes, triolein, electrical impedance spectroscopy (EIS), lipase sensor, neutron reflectometry*

INTRODUCTION

Lipases are versatile enzymes due to their ability to hydrolyze carboxylic ester bonds, catalyze esterification, nonaqueous transesterification reactions, and interesterification.[1] Lipases derived from animal, plant, and microbial sources are of great interest to many medical, pharmaceutical, and detergent companies.[2] As an example of a medical application, the diagnosis and management of patients with acute pancreatitis could be achieved by measuring the activity of circulating lipases in blood serum.[3,4] As 10% of marketed enzymes around the world are lipases, a rapid in-line assay to monitor reaction kinetics during production would also be of benefit as a quality control procedure.[5]

To date, many current lipase activity assays rely on measuring surrogate markers such as changes in ionic concentration, pH, particle aggregation, fluorescence, or other optical properties in the surrounding medium of a lipase−lipid mixture. Inevitably, they involve the use of additional chemical components to provide a signal which can increase costs and limit sensitivity.[6−9] Measuring the direct effect of lipases on lipid substrates using amperometric methods has also been described,[10,11] but the techniques typically require a time-consuming lipid substrate deposition methodology that might also include the deposition of nanocomposites and other conductive materials and/or include the use of toxic solvents such as chloroform.[12] Other techniques that rely on lengthy lipid substrate deposition processes include the use of quartz crystal microbalance, sum-frequency generation vibrational spectroscopy, and atomic force microscopy.[13−16]

Here, we present a sensor for the detection of lipase activity using a tethered triglyceride substrate that is self-assembled using a rapid solvent exchange technique. This involves a wash step that converts the lipids from being dissolved in an ethanolic mobile phase to an aqueous solution where the presence of the hydrophobic moieties of the lipids dictates they must form into anisotropic layer(s) around the tethering molecules. The sensor uses the same tethering molecules used to form sparsely tethered bilayer lipid membranes (tBLMs).[17] When used with electrical impedance spectroscopy (EIS), this sparsely tethered lipid membrane enables a direct and real-time measurement of lipase enzymatic activity.

Triglyceride molecules typically do not spontaneously form into bilayer lipid membranes. This is most likely due to their molecular shape not being appropriate to form planar structures. However, we hypothesized that the use of hydrophobic anchoring molecules, or tethers, might be able to form a support around which triglycerides can associate to create a stable membrane layer. Factors such as the lipid chain length and degree of saturation are critical in determining the

Received: August 9, 2023
Revised: October 9, 2023
Accepted: October 12, 2023
Published: November 6, 2023

suitability of a triglyceride for this purpose. The triglyceride triolein, which possesses three C18 fatty acid chains with double bonds at the 9−11 position, was chosen (Figure 1) as

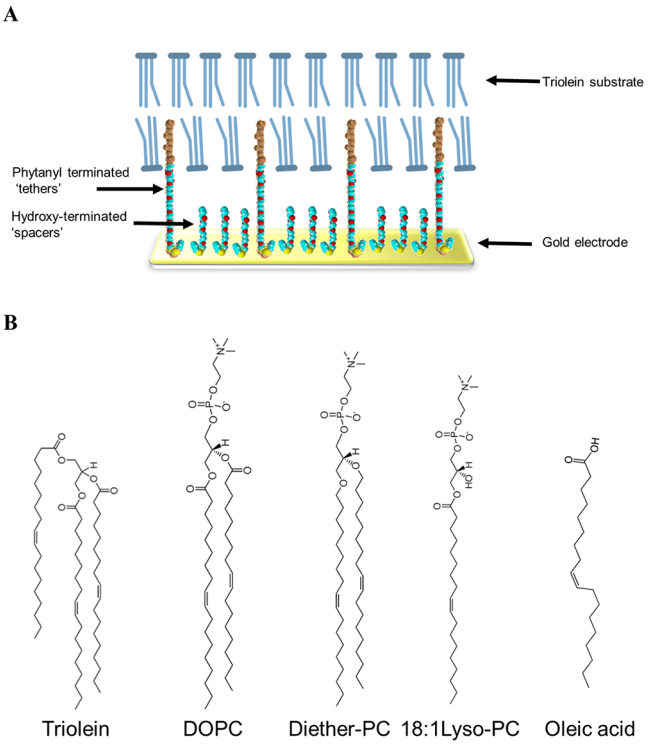

Figure 1. (A) Cartoon depicting the triolein-tethered membrane as a bilayer. (B) Chemical structures of the substrates used in this study, namely, triolein, DOPC, diether-PC, 18:1Lyso-PC, and oleic acid.

triolein is similar in length and composition to phospholipids such as dioleoylphosphatidylcholine (DOPC) widely represented in mammalian membranes. The product of enzymatic hydrolysis of triolein is oleic acid, which, as will be demonstrated, seems to persist in the membrane and does not cause membrane disintegration.

We confirm the effectiveness of the sensor by comparing lipase activities in the presence and absence of inhibitors and by using varying lipid substrate mixtures. We then further demonstrate that it is unresponsive to phospholipase A_2 activity that could also be present in biological solutions. Finally, we analyzed the structure of the tethered membrane using neutron reflectometry.

EXPERIMENTAL SECTION

Buffers and Enzymes. Unless stated otherwise, experiments were performed in the presence of 10 mM Tris-buffered 100 mM NaCl solutions at pH 7 (referred to as tris buffer). Where appropriate, this buffer was supplemented with 1 mM $CaCl_2$ to increase the activity of the phospholipases. Porcine pancreatic lipase (PPL), the pancreatic lipase inhibitor *orlistat* (tetrahydrolipstatin), porcine pancreatic phospholipase A_2 (PLA_2), recombinant PLA_1 from *Aspergillus oryzae*, and lipase from *Candida rugosa* were all purchased from Sigma-Aldrich Australia.

Tethered Membrane Substrate Formation. Tethered membranes were prepared using precoated 25 mm × 75 mm gold on polycarbonate slides containing no metal intermediate layers from SDx Tethered Membranes Pty Ltd., Roseville, NSW, Australia. These slides consist of six 2.1 mm^2, patterned, gold-sputtered electrodes each with a surface roughness ≈1 nm. These were coated with 10 mol % tether molecules comprising 4-methyl phytanyl hydrophobic chains conjugated to 11-oxygen ethylene glycol linkers interspersed with 90 mol % hydroxy-terminated 8-oxygen ethylene glycol *spacer* molecules (Figure 1A). The tether and spacer molecules create a reservoir region for ions between the bilayer membrane and the gold electrode. To the anchoring chemistries, a second layer of 3 mM mobile phase lipids in ethanol is added for exactly 2 min. Following this, each membrane is rapidly solvent exchanged by washing out the mobile phase lipids with 3 × 400 μL tris buffer to enable the lipids to self-assemble into a membrane around the tether moieties.[18,19] Three different mobile phase lipids were used to create the tethered lipid substrates (Figure 1B), namely: the triglyceride triolein ((1,2,3-tri-(9Z-octadecenoyl)-glycerol), the ester phospholipid DOPC (1,2-dioleoyl-sn-glycero-3-phosphocholine), and a diether phospholipid with a structure, akin to DOPC, designated diether-PC (1,2-di-O-(9Z-octadecenyl)-sn-glycero-3-phosphocholine). In these experiments, because it lacks any hydrolizable ester groups, diether-PC is used to create negative control tethered membrane substrates.[17] Experiments looking into mixtures of triolein with single-chained lipids included the use of 18:1 Lyso-PC (1-oleoyl-2-hydroxy-sn-glycero-3-phosphocholine; Avanti Polar Lipids, USA) and Oleic acid ((9Z)-Octadec-9-enoic acid; Sigma-Aldrich, Australia).

Electrical Impedance Spectroscopy (EIS). Impedance measurements were done using a TethaPod swept-frequency electrical impedance spectrometer (SDx Tethered Membranes, Pty Ltd.). AC potentials at 25 mV amplitude were applied at frequencies ranging from 0.1 to 2000 Hz. Data were fitted to an equivalent circuit consisting of a resistor/capacitor circuit, representing the tethered membrane, in series with a constant phase element representing the imperfect capacitance of the tethering gold electrode, and a resistor to represent the impedance of the surrounding electrolyte solution, as described previously.[20] Impedance magnitude and phase data were fitted using a proprietary adaptation of a Levenberg−Marquardt fitting routine incorporated into the TethaQuick software (SDx Tethered Membranes Pty Ltd.).

For ease of comprehension, membrane resistance (R_m) values are reported as membrane conductance, G_m, where $G_m = 1/R_m$. Conductance changes over time were then normalized by dividing the G_m values by an appropriately designated baseline control value. Control buffer washes were performed prior to the addition of lipases to ensure there was no nonspecific drift in G_m.

Neutron Reflectometry (NR) and Data Fitting. Located at the 20 MW OPAL research reactor (Australian Nuclear Science and Technology Organisation (ANSTO), Sydney, Australia), NR data were collected using the SPATZ time-of-flight instrument.[21] This instrument is located on a cold neutron guide and as such is supplied with a neutron bandwidth ranging from 2.5 to 18.0 Å with the cutoff being determined by the instrument disc choppers. The Q resolution of the experiment was set at $\Delta Q/Q$ of 3.3% where Q, the scattering vector, is defined as

$$Q = (4\pi\sin\theta)/\lambda$$

where θ is the scattering angle and λ is the wavelength of the incident radiation. Incident angles of 0.5°, 0.85°, and 3.8° were used with the data spliced together after normalization to the direct beam and background subtraction to produce a single absolutely scaled reflectivity data set over a Q range of 0.006 to 0.25 $Å^{-1}$ using *refnx* reflectometry analysis package.[22]

Tethered membranes were formed on 50 mm diameter, 7 mm thick silicon disks that had been coated with chromium and then gold at the Australian National Fabrication Facility, ANU node. These disks were left to incubate in an ethanolic solution containing the T10 tethering chemistries (see tethered membrane section above) for at least 1 h. Following this, a mobile lipid second layer of either DOPC or triolein (3 mM in ethanol) was allowed to incubate on the disks for 20 min. This was followed by a rapid solvent exchange with Tris buffer to enable the self-assembly of the tethered membrane.[23] Coated disks were clamped to a bespoke perfusion chamber for tethered membrane assembly and measurement at the SPATZ sample position.

Neutron contrast within the samples was achieved via the use of hydrogenous phospholipids and deuterated triolein (produced by the

https://doi.org/10.1021/acsami.3c11767
ACS Appl. Mater. Interfaces 2023, 15, 52237−52243

National Deuteration Facility, ANSTO) with further contrast provided by bathing solutions of tris buffer in either D_2O, H_2O, or HDO mixtures that nominally match the neutron scattering length density (SLD) of the gold layer.

The absolutely scaled data sets were modeled using *refnx*,[24] a python package for generalized curving fitting analysis for X-ray and neutron reflectometry data. NR data were fitted using "slabs" with four main parameters for all the layers: SLD, thickness, roughness, and water volume fraction.

RESULTS AND DISCUSSION

The Bode plots comparing triolein-tethered membranes with traditional phospholipid tBLMs show a frequency-at-minimum-phase at higher frequencies and a phase-at-minimum-phase at a lower angle (Figure 2). The former suggests that triolein-tethered membranes show less ionic transport resistance than do phospholipid tBLMs. That the phase-at-minimum-phase for triolein is lower than the PC membranes indicates that either the capacitance of the tethering electrode is lower and/or the capacitance of the membrane is higher than the PC membranes.[25]

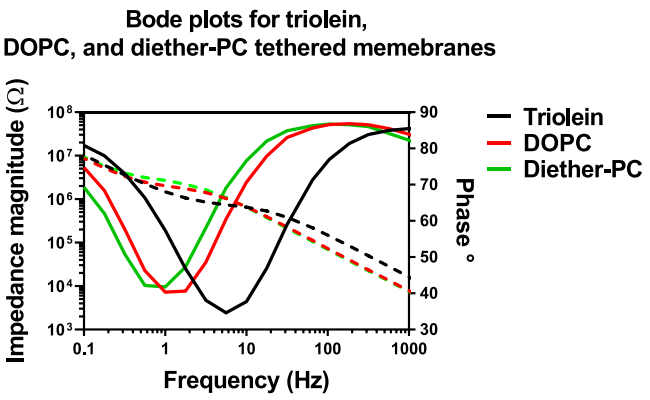

Figure 2. Typical Bode plots of a triolein-tethered membrane in comparison to phospholipid tBLMs composed of DOPC or diether-PC lipids. Dashed lines represent frequency versus impedance magnitude, while solid lines are frequency versus phase angle plots.

When fitted to an equivalent circuit (see Table 1), the triolein membranes show a reduced imperfect capacitance (Q_s) at the tethering electrode-reservoir region than the phospholipid membranes, yet the constant phase element dimensional constant (α_s) is similar for all membranes. α_s indicates the contribution of the restricted diffusion in the reservoir region.[25,26] That they are similar suggests that triolein molecules are not interfering with ionic transport in the reservoir following self-assembly any more or less than phospholipids do. The relatively low membrane capacitance (C_m) of 0.64 μF cm^{-2} for the triolein-tethered membrane compared to the phospholipid tBLMs suggests a thicker membrane and/or a membrane with less water content.

The ability of the triolein-tethered membrane sensor to detect lipase activity is demonstrated in Figure 3A. The pancreatic lipase inhibitor, orlistat, forms a covalent bond with a serine residue in the enzyme's active site.[27,28] The absence of any change in membrane conduction in the presence of orlistat confirms that membrane conduction changes are due to the catalytic actions of the enzyme and not to the protein inserting itself into the membrane. This is further demonstrated in Figure 3B, where the lipase shows no activity on phospholipid tBLM substrates, even without the inhibitor. Figure 3C shows the triolein-tethered membrane response to the enzymes PLA_1 and phospholipase PLA_2. While there is no response to the inflammatory enzyme PLA_2, the substrate responds to PLA_1. This is in agreement with previous studies that demonstrated PLA_1 has activity against 1,3 triglycerides as well as phospholipids.[29]

From the Bode plots (see Supporting Information Figure S1), it can be seen that a well-sealed membrane exists and persists following enzymatic hydrolysis of 100% triolein-tethered membranes, albeit with higher membrane conduction. This is to be contrasted with previous studies using phospholipid tBLMs exposed to phospholipases.[17] When the membrane seal is eliminated, the Bode diagrams would show no minimum in the phase plot, and the apparent conduction (G_m) values dramatically increase beyond the relevance of the model from which these measures are derived. These data suggest that the oleic acids formed from the triglyceride hydrolysis are not sequestering themselves out of the membrane and any alterations in membrane conduction are solely due to a rearrangement of the packing of the lipid molecules. To explore this further, we created tethered bilayers of triolein with differing ratios of phospholipid (DOPC), lysolipids, and fatty acids. The hypothesis is that we could alter the overall critical packing parameter (CPP)[30] of the membrane in such a way that membrane disintegration is made possible as a result of triglyceride hydrolysis. When differing proportions of double-chained phospholipid were used (DOPC), there was no difference in the response to the enzyme if the ratio of triglyceride:phospholipid was greater

Table 1. Typical Fitted Parameters for Triolein, DOPC, and Diether-PC Tethered Membranes According to the Equivalent Circuit Depicted Below[a]

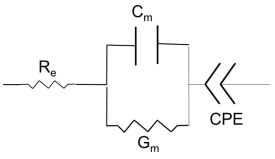

membranes	R_e, Ω	Q_s, μF cm^{-2}	α_s	G_m, μS	C_m, μF cm^{-2}
triolein	462 ± 52.4	7.4 ± 0.32	0.9 ± 0.02	2.2 ± 0.55	0.64 ± 0.07
DOPC	245 ± 72	8.6 ± 0.6	0.9 ± 0.03	0.45 ± 0.03	1.22 ± 0.16
diether-PC	372 ± 45	9.9 ± 1.4	0.89 ± 0.02	0.49 ± 0.17	1.46 ± 0.19

[a] R_e = electrolyte resistance, Q_s = imperfect capacitance of reservoir region, α_s = dimensional constant of CPE of reservoir region, G_m = membrane conductance, and C_m = membrane capacitance. Each value is the mean plus the standard deviation of six separate tethered membranes formed by the solvent exchange method.

https://doi.org/10.1021/acsami.3c11767
ACS Appl. Mater. Interfaces 2023, 15, 52237−52243

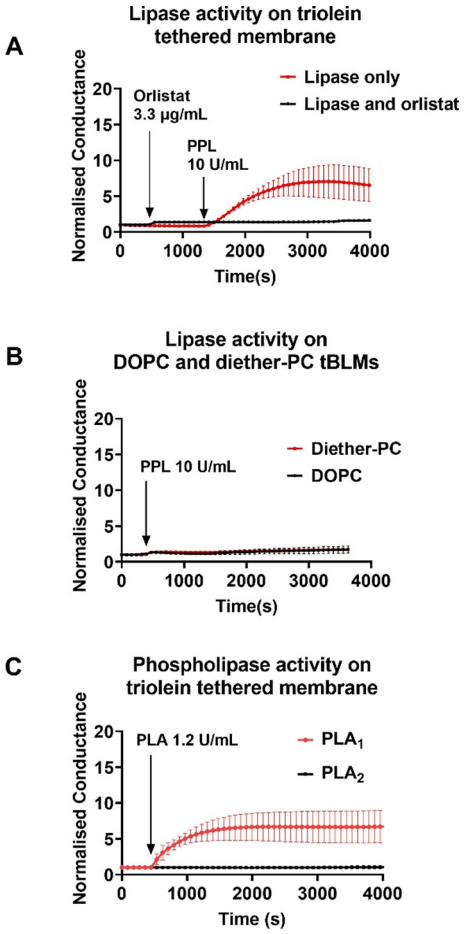

Figure 3. Membrane conduction changes due to the addition of lipases on the triolein-tethered membrane and phospholipid tBLM substrates. (A) Addition of 10 U/mL porcine pancreatic lipase (PPL) to triolein-tethered membranes in the presence (n = 3) and absence (n = 3) of 3.3 μg/mL lipase inhibitor, *orlistat*. Lipase activity is visible in the form of membrane conductance changes in the absence of the inhibitor. (B) In contrast to the triolein-tethered membranes, PPL exhibits no activity of phospholipid tBLMs comprising DOPC (n = 3) or diether-PC (n = 3), as expected. (C) Phospholipase A_2 shows no sign of inducing hydrolysis of triolein-tethered membrane substrates (n = 3). Interestingly, however, phospholipase A_1 enzymes show significant catalytic activity on these substrates (n = 3).

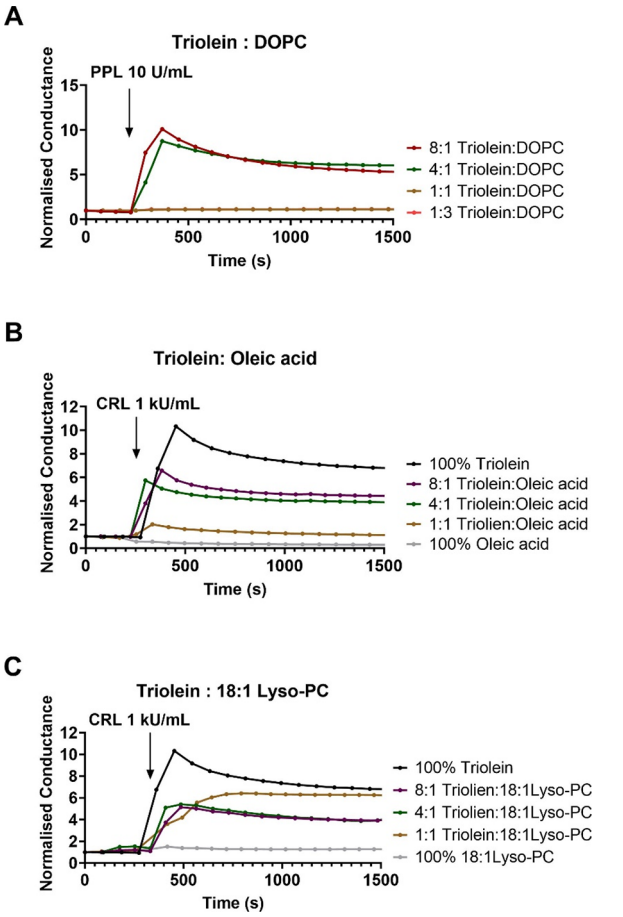

Figure 4. Membrane conduction changes due to the addition of lipases on tethered membranes formed with triolein and phospholipid or fatty acid mixtures. (A) Responses (or lack of responses) to the addition of porcine pancreatic lipase (PPL) to varying mixtures of triolein and DOPC suggest that self-assembly of the triglycerides with double-chained phospholipids will favor one lipid type over the other, depending on their relative quantities. In contrast, the incorporation of single-chained lipids reduces the response to Candida rugosa lipase (CRL) roughly proportional to (B) proportion of oleic acid present or (C) proportion of 18:1 Lyso-PC present. All figures are the mean of n = 3 tethered membranes; for clarity purposes, the error bars are not shown. Proportions are calculated as mol:mol.

than one; and no response at all if the ratio was 0.5 or less (Figure 4A). This confirms that triglycerides and phospholipids cannot be mixed in such high proportions to create lipid bilayers.[31,32] It also shows that self-assembly around the tethering molecules will favor one of these lipid types over the other depending on their relative proportions in the ethanolic seed solution prior to solvent exchange.

We also wanted to trial an industrially produced lipase on triolein-tethered bilayers with and without single-chain fatty acids. For this, we used lipase produced by the yeast *Candida rugosa*. Interestingly, the incorporation of single-chained lipids (18:1 Lyso-PC and oleic acid) only resulted in a reduction in the peak response to the *Candida rugosa* lipase (CRL) that is roughly proportional to the amount of the single-chained lipids in the tethered bilayer (Figure 4B,C). These data are further confirmation that the electrical impedance response to the lipases is dependent on the amount of substrate available and not as a result of the lipase proteins themselves partitioning into the membrane. Over time, as the triglyceride molecules are hydrolyzed, the ratio of single-chained fatty acids to the residual triglycerides will result in new packing geometries being formed. Some of these geometries may reduce the probability of membrane-spanning defects and, consequently, a reduced membrane conduction, as seen in Figure 4A–C. Other mechanisms that can cause a decrease in membrane conduction include the effect of lowering the pH. This will be associated with an increase in the fatty acid content. A pH-dependent drop in bilayer conduction has previously been reported and is proposed to be a result of increased membrane packing due to increased hydrogen bonding at the lipid–water interface in phospholipid[33,34] and fatty acid membranes.[35]

Key to the sensitivity of the sensor is the presence of an aqueous reservoir region between the tethering electrode and the triglyceride membrane. The reservoir enables sufficient space between the tethering gold electrode and the membrane for ions to traverse into and out of when an alternating current (AC) voltage is applied. Without a reservoir, the migration of ions across the membrane will be inadequate, and this will

https://doi.org/10.1021/acsami.3c11767
ACS Appl. Mater. Interfaces 2023, 15, 52237–52243

appear as an additional resistance in series with the membrane resistance, resulting in a lower conduction change in response to the enzyme. Another factor that could influence the sensor's sensitivity is the membrane thickness. Should the triglycerides coalesce around the tethers in multilamellar structures, the increased overall thickness will also impede the flow of ions and decrease membrane conduction. So, to verify the tethered triglyceride architecture, neutron reflectometry was employed. Figure 5 shows the relative thicknesses of a deuterated triolein-

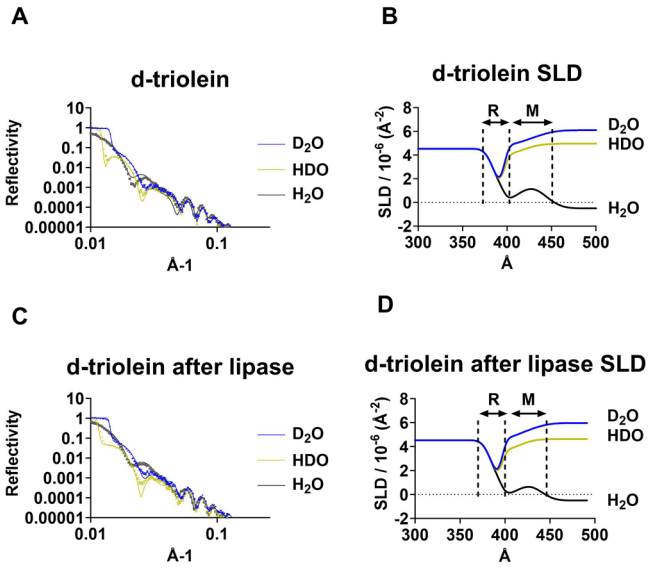

Figure 5. Neutron reflectometry of a deuterated triolein-tethered membrane. (A) Neutron reflectivity of the membrane using three different contrasts, namely, D_2O, a gold-matched mixture of D_2O and H_2O (HDO) and H_2O. (B) Scattering length density (SLD) versus distance calculated from the data in A. "R" is the reservoir region (~30 Å) between the gold substrate and the membrane, "M" (~50 Å). (C) Neutron reflectivity of the membrane following the addition of 10 U/mL porcine pancreatic lipase. (D) SLD plot derived from the same data. As in B, "R" is the reservoir region (~30 Å) between the gold substrate and the membrane, "M" (~50 Å).

tethered membrane before and after the addition of PPL. The SLD versus distance plots reveal a reservoir region of ~30 Å and a membrane that is ~50 Å thick. This is in agreement with the low membrane capacitance values (0.64 μF cm^{-2}, Table 1) which suggests triolein forms thicker tethered membranes than DOPC tBLMs. Using neutron reflectometry, we also measured DOPC tBLMs, and their calculated membrane thickness was ~40 Å (see Supporting Information Figure S2). However, these data need to be treated with caution as the overall membrane coverage on the substrates used for neutron reflectometry, using the d-triolein, was calculated to be 50%. We repeated the experiment with hydrogenated triolein, which yielded a better overall coverage (90%), but the triglyceride seemed to be spread very thin, with a thickness of ~13 Å (see Supporting Information Figure S3). These disparities might be explained by the relative size of the substrates used in neutron reflectometry experiments (~2000 mm^2 compared to 2.1 mm^2 for EIS measures). The self-assembly of triglyceride molecules around sparsely distributed tethering molecules over large areas will inevitably be inconsistent. Figure 5C,D indicates that the membrane remains unaltered after the addition of hydrogenated lipase protein, suggesting that the lipase is not incorporating itself into or adsorbing onto the membrane. It also confirms that the tethered membrane structure remains intact despite enzymatic hydrolysis. However, in the h-triolein samples (see Supporting Information Figure S2C,D), there is evidence of membrane swelling after addition of lipase, probably due to incorporation of the bathing solution as a result of lipase hydrolysis. The impact of this effect might not have been evident in the d-triolein samples due to the relatively low surface coverage. To support this view, we demonstrated that d-triolein-tethered membranes can be produced using the solvent exchange technique in tris buffer made with D_2O and respond to PPL when measured using EIS (see Supporting Information Figure S4).

CONCLUSIONS

These tethered membrane lipase sensors can be assembled in under 15 min. Further, following preparation, they can be stored for days at a time and remain intact and functional. That triolein-tethered membranes remain a bilayer following exposure to lipases is an example of the critical balance of free energies. These include the steric packing of lipids, the entropy of the interfacial water, maximized by excluding the methylene chains from water, and direct hydrogen bonding of the polar groups to the water in the bathing solution. This balance governs whether an amphiphile will form a bilayer, a micelle, or a more complex hexagonal or cubic phase. Homogeneous dispersions of lysophospholipids and fatty acid compounds do not typically form bilayers. However, when mixed, the free energy balance can result in a bilayer forming[36] which enables the creation of a stable sensor substrate for measuring lipase activity in real time.

ASSOCIATED CONTENT

Supporting Information

The Supporting Information is available free of charge at https://pubs.acs.org/doi/10.1021/acsami.3c11767.

Bode plot and capacitance plots for lipase affected triolein-tethered membranes; neutron reflectometry for DOPC; hydrogenated triolein-tethered membranes; and membrane conductance response to lipase hydrolysis of a deuterated triolein-tethered membrane in D_2O (PDF)

AUTHOR INFORMATION

Corresponding Author

Charles G. Cranfield − *School of Life Sciences, University of Technology Sydney, Ultimo, NSW 2007, Australia;* orcid.org/0000-0003-3608-5440; Email: Charles.cranfield@uts.edu.au

Authors

Upeksha Mirissa Lankage − *School of Life Sciences, University of Technology Sydney, Ultimo, NSW 2007, Australia*

Stephen A. Holt − *School of Life Sciences, University of Technology Sydney, Ultimo, NSW 2007, Australia; Australian Nuclear Science and Technology Organisation, Lucas Heights, NSW 2234, Australia;* orcid.org/0000-0003-3189-8047

Samara Bridge − *School of Life Sciences, University of Technology Sydney, Ultimo, NSW 2007, Australia*

Bruce Cornell − *School of Life Sciences, University of Technology Sydney, Ultimo, NSW 2007, Australia; SDx Surgical Diagnostics Pty Ltd., Roseville, NSW 2069, Australia*

Complete contact information is available at: https://pubs.acs.org/10.1021/acsami.3c11767

Author Contributions

The project was conceived by C.G.C. and B.C. U.M.L. led the experiments and was assisted by S.B. Neutron reflectometry and data fitting were done with the assistance of S.A.H. C.G.C., S.A.H., and B.C. wrote the manuscript.

Notes

The authors declare the following competing financial interest(s): Declaration of interest: Bruce Cornell is a shareholder and employee of SDx Surgical Diagnostics Pty Ltd.

■ ACKNOWLEDGMENTS

This study was supported by the ARC Research Hub for Integrated Device for End-user Analysis at Low-levels (IDEAL) (IH150100028). We acknowledge the support of the Australian Centre for Neutron Scattering, ANSTO, and the Australian Government through the National Collaborative Research Infrastructure Strategy, in supporting the neutron research infrastructure used in this work via ACNS proposals P9765, DB13297, and NDF9783.

■ REFERENCES

(1) Houde, A.; Kademi, A.; Leblanc, D. Lipases and Their Industrial Applications. *Appl. Biochem. Biotechnol.* **2004**, *118* (1), 155−170.
(2) Herrera-López, E. J. Lipase and Phospholipase Biosensors: A Review. *Lipases Phospholipases* **2012**, *861*, 525−543.
(3) Agarwal, N.; Pitchumoni, C.; Sivaprasad, A. Evaluating Tests for Acute Pancreatitis. *Am. J. Gastroenterol.* **1990**, *85* (4), 356−366.
(4) Treacy, J.; Williams, A.; Bais, R.; Willson, K.; Worthley, C.; Reece, J.; Bessell, J.; Thomas, D. Evaluation of Amylase and Lipase in the Diagnosis of Acute Pancreatitis. *ANZ J. Surg.* **2001**, *71* (10), 577−582.
(5) Guerrand, D. Lipases Industrial Applications: Focus on Food and Agroindustries. *OCL* **2017**, *24* (D403), 2017.
(6) Pohanka, M. Biosensors and Bioassays Based on Lipases, Principles and Applications, a Review. *Molecules* **2019**, *24* (3), 616−630.
(7) Hussain, Z.; Zafiu, C.; Küpcü, S.; Pivetta, L.; Hollfelder, N.; Masutani, A.; Kilickiran, P.; Sinner, E.-K. Liquid Crystal Based Sensors Monitoring Lipase Activity: A New Rapid and Sensitive Method for Cytotoxicity Assays. *Biosens. Bioelectron.* **2014**, *56*, 210−216.
(8) Starodub, N. Biosensors for the Evaluation of Lipase Activity. *J. Mol. Catal. B: Enzym.* **2006**, *40* (3−4), 155−160.
(9) Sandoval, G.; Herrera-López, E. J. Lipase, Phospholipase, and Esterase Biosensors. In *Lipases and Phospholipases*; Springer, 2018; pp 391−425.
(10) Narang, J.; Pundir, C. Construction of a Triglyceride Amperometric Biosensor Based on Chitosan−Zno Nanocomposite Film. *Int. J. Biol. Macromol.* **2011**, *49* (4), 707−715.
(11) Solanki, S.; Pandey, C. M.; Soni, A.; Sumana, G.; Biradar, A. M. An Amperometric Bienzymatic Biosensor for the Triglyceride Tributyrin Using an Indium Tin Oxide Electrode Coated with Electrophoretically Deposited Chitosan-Wrapped Nanozirconia. *Microchim. Acta* **2016**, *183* (1), 167−176.
(12) Mirsky, V. M.; Krause, C.; Heckmann, K. D. Capacitive Sensor for Lipolytic Enzymes. *Thin Solid Films* **1996**, *284*, 939−941.
(13) Jackman, J. A.; Cho, N.-J.; Duran, R. S.; Frank, C. W. Interfacial Binding Dynamics of Bee Venom Phospholipase A2 Investigated by Dynamic Light Scattering and Quartz Crystal Microbalance. *Langmuir* **2010**, *26* (6), 4103−4112.
(14) Kai, S.; Li, X.; Li, B.; Han, X.; Lu, X. Calcium-Dependent Hydrolysis of Supported Planar Lipids Was Triggered by Honey Bee Venom Phospholipase a 2 with the Right Orientation at the Interface. *Phys. Chem. Chem. Phys.* **2018**, *20* (1), 63−67.
(15) Zhang, F.; Li, X.; Ma, Y.; Wang, C.; Hu, P.; Wang, F.; Lu, X. Illustrating Interfacial Interaction between Honey Bee Venom Phospholipase A2 and Supported Negatively Charged Lipids with Sum Frequency Generation and Laser Scanning Confocal Microscopy. *Langmuir* **2020**, *36* (11), 2946−2953.
(16) Hong, C. Y.; Han, C.-T.; Chao, L. Nonspecific Binding Domains in Lipid Membranes Induced by Phospholipase A2. *Langmuir* **2016**, *32* (27), 6991−6999.
(17) Garcia, A.; Deplazes, E.; Aili, S.; Padula, M. P.; Touchard, A.; Murphy, C.; Mirissa Lankage, U.; Nicholson, G. M.; Cornell, B.; Cranfield, C. G. Label-Free, Real-Time Phospholipase-a Isoform Assay. *ACS Biomater. Sci. Eng.* **2020**, *6* (8), 4714−4721.
(18) Tamm, L. K.; McConnell, H. M. Supported Phospholipid Bilayers. *Biophys. J.* **1985**, *47* (1), 105−113.
(19) Alghalayini, A.; Garcia, A.; Berry, T.; Cranfield, C. G. The Use of Tethered Bilayer Lipid Membranes to Identify the Mechanisms of Antimicrobial Peptide Interactions with Lipid Bilayers. *Antibiotics* **2019**, *8* (1), 12.
(20) Cranfield, C. G.; Henriques, S. T.; Martinac, B.; Duckworth, P. A.; Craik, D. J.; Cornell, B. Kalata B1 and Kalata B2 Have a Surfactant-Like Activity in Phosphatidylethanolomine Containing Lipid Membranes. *Langmuir* **2017**, *33* (26), 6630−6637.
(21) Le Brun, A. P.; Huang, T.-Y.; Pullen, S.; Nelson, A. R.; Spedding, J.; Holt, S. A. Spatz: The Time-of-Flight Neutron Reflectometer with Vertical Sample Geometry at the Opal Research Reactor *J. Appl. Crystallogr.* 2023, *56*(1), 18, DOI: 10.1107/S160057672201086X
(22) Nelson, A. R.; Prescott, S. W. Refnx: Neutron and X-Ray Reflectometry Analysis in Python. *J. Appl. Crystallogr.* **2019**, *52* (1), 193−200.
(23) Yepuri, N. R.; Holt, S. A.; Moraes, G.; Holden, P. J.; Hossain, K. R.; Valenzuela, S. M.; James, M.; Darwish, T. A. Stereoselective Synthesis of Perdeuterated Phytanic Acid, Its Phospholipid Derivatives and Their Formation into Lipid Model Membranes for Neutron Reflectivity Studies. *Chem. Phys. Lipids* **2014**, *183*, 22−33.
(24) Holt, S. A.; Oliver, T. E.; Nelson, A. R. Using Refnx to Model Neutron Reflectometry Data from Phospholipid Bilayers. In *Membrane Lipids*; Springer, 2022; pp 179−197.
(25) Cranfield, C. G.; Bettler, T.; Cornell, B. Nanoscale Ion Sequestration to Determine the Polarity Selectivity of Ion Conductance in Carriers and Channels. *Langmuir* **2015**, *31*, 292−298.
(26) Krishna, G.; Schulte, J.; Cornell, B. A.; Pace, R.; Wieczorekt, L.; Osman, P. D. Tethered Bilayer Membranes Containing Ionic Reservoirs: The Interfacial Capacitance. *Langmuir* **2001**, *17*, 4858−4866.
(27) Lengsfeld, H.; Wolfer, H. Inhibition of Pancreatic Lipase in Vitro by the Covalent Inhibitor Tetrahydrolipstatin. *Biochem. J.* **1988**, *256* (2), 357−361.
(28) Heck, A. M.; Yanovski, J. A.; Calis, K. A. Orlistat, a New Lipase Inhibitor for the Management of Obesity. *Pharmacotherapy: The Journal of Human Pharmacology and Drug. Therapy* **2000**, *20* (3), 270−279.
(29) Xin, R.; Khan, F. I.; Zhao, Z.; Zhang, Z.; Yang, B.; Wang, Y. A Comparative Study on Kinetics and Substrate Specificities of Phospholipase A1 with Thermomyces Lanuginosus Lipase. *J. Colloid Interface Sci.* **2017**, *488*, 149−154.
(30) Israelachvili, J. N.; Mitchell, D. J.; Ninham, B. W. Theory of Self-Assembly of Hydrocarbon Amphiphiles into Micelles and Bilayers. *J. Chem. Soc, Faraday Trans. 2* **1976**, *72*, 1525−1568.
(31) Hamilton, J. A. Interactions of Triglycerides with Phospholipids: Incorporation into the Bilayer Structure and Formation of Emulsions. *Biochemistry* **1989**, *28* (6), 2514−2520.
(32) Pakkanen, K. I.; Duelund, L.; Qvortrup, K.; Pedersen, J. S.; Ipsen, J. H. Mechanics and Dynamics of Triglyceride-Phospholipid Model Membranes: Implications for Cellular Properties and Function. *Biochim. Biophys. Acta, Biomembr.* **2011**, *1808* (8), 1947−1956.

(33) Cranfield, C. G.; Berry, T.; Holt, S. A.; Hossain, K. R.; Le Brun, A. P.; Carne, S.; Al Khamici, H.; Coster, H.; Valenzuela, S. M.; Cornell, B. Evidence of the Key Role of H3o+ in Phospholipid Membrane Morphology. *Langmuir* **2016**, *32* (41), 10725−10734.
(34) Deplazes, E.; Poger, D.; Cornell, B.; Cranfield, C. G. The Effect of Hydronium Ions on the Structure of Phospholipid Membranes. *Phys. Chem. Chem. Phys.* **2018**, *20* (1), 357−366.
(35) Lowe, L. A.; Kindt, J. T.; Cranfield, C.; Cornell, B.; Macmillan, A.; Wang, A. Subtle Changes in Ph Affect the Packing and Robustness of Fatty Acid Bilayers. *Soft Matter* **2022**, *18* (18), 3498−3504.
(36) Jain, M.; Van Echteld, C.; Ramirez, F.; De Gier, J.; De Haas, G.; Van Deenen, L. Association of Lysophosphatidylcholine with Fatty Acids in Aqueous Phase to Form Bilayers. *Nature* **1980**, *284*, 486−487.

https://doi.org/10.1021/acsami.3c11767
ACS Appl. Mater. Interfaces 2023, 15, 52237−52243